J. Med. Biol. Eng. (2015) 35:517–527
DOI 10.1007/s40846-015-0065-0

ORIGINAL ARTICLE

Wake/Sleep Identification Based on Body Movement for Parkinson's Disease Patients

Xing Qian[1] · Hongwei Hao[1] · Ying Chen[1] · Luming Li[1]

Received: 21 May 2014 / Accepted: 25 January 2015 / Published online: 14 August 2015

Abstract This paper presents a method for identifying a patient's wake/sleep state for closed-loop deep brain stimulation (DBS). The method uses a real-time wake/sleep identification algorithm that includes posture analysis based on the movement of the chest below the clavicle, which is the location of the subcutaneous pulse generator. A single micro-accelerometer was used to monitor the movement of the wrist and the chest of thirteen healthy adults and twelve patients with Parkinson's disease for nine continuous hours. The wake/sleep state identification for the chest algorithm had accuracy, sensitivity, and specificity values of 85.78, 84.21, and 82.08 %, respectively, compared to video recordings for patients with DBS ON, and 82.74, 82.68, and 82.28 %, respectively, for patients with DBS OFF. The algorithm performance for the chest is comparable to that of the commonly used location on the wrist. The real-time wake/sleep identification algorithms were proved to be effective. This research provides a practical method for closed-loop DBS, which will greatly benefit patients with Parkinson's disease.

Keywords Parkinson's disease · Deep brain stimulation (DBS) · Wake/sleep identification · Body movement · Accelerometer

✉ Luming Li
lilm@tsinghua.edu.cn

1 School of Aerospace, Tsinghua University, Beijing 100084, China

1 Introduction

Deep brain stimulation (DBS) is a key therapy used to treat Parkinson's disease (PD). A deep brain stimulator consists of an implantable pulse generator, one or two stimulating leads, and one or more extensions. However, there are two major disadvantages to this open-loop stimulation design. One is the side effects of the continuous high-frequency electrical pulses on neural nuclei [1, 2]. The other is the limited battery life of the pulse generator. Each implanted battery has an expected lifetime of about 5 years [3], with battery replacement surgery needed when the battery is exhausted. Thus, patients with PD would greatly benefit from a closed-loop device that could automatically adapt the stimulation according to the patient's condition rather than over-stimulating the brain.

Brain waves are a direct, reliable indicator of patient symptoms. However, the collection and subsequent analysis of electroencephalogram (EEG) signals require a large amount of medical equipment, which makes it difficult to integrate with current deep brain stimulators, since an implantable device must be very small. The inability to measure brain waves impedes the development of closed-loop DBS.

Clinical observations have suggested another way to implement closed-loop DBS. Tremor, one of the major symptoms for patients with PD, disappears during sleep [4], so patients do not need as much stimulation in the sleep state as in the wake state. Therefore, DBS can be modified depending on the wake/sleep state of the patient.

A literature survey revealed that body movements provide simple, reliable feedback information that can be used to identify an individual's wake/sleep state. Noncontact methods to measure body movement include those that use pneumatic cushions [5], piezoelectric films [6], and video cameras [7]. However, an additional communication module is needed to transmit the identified wake/sleep state for such noncontact methods, which would constrain the patient's daily life. Actigraphy, which collects acceleration data from the wrist, gives better non-real-time wake/sleep analysis results than does polysomnography (PSG) [8, 9]. The first actigraphic algorithm for wake/sleep analysis was proposed by Webster et al. [10], who established a foundation for later wake/sleep identification algorithms. Actigraphy research has continued for 30 years [11–14]. A study by Sadeh et al. [15] had overall agreement rates with PSG of 91–93 %. However, no feasible applications of closed-loop deep brain stimulators have been reported. The development of a real-time algorithm for wake/sleep identification and the validation of the algorithm on PD patients will greatly promote the design of closed-loop DBS.

This study describes an effective method for identifying a patient's wake/sleep state in real time for closed-loop DBS. The real-time wake/sleep identification algorithm uses posture analysis based on the movement of the chest below the clavicle, where the pulse generator is implanted subcutaneously. A single micro-accelerometer was used to sense movements of the wrist and the chest of nine healthy young adults, four healthy old people, and twelve patients with PD for nine continuous hours. The performance of the chest algorithm was comparable to that of the commonly used location on the wrist. Both the miniature accelerometer and the effective real-time wake/sleep identification algorithm can be used in closed-loop DBS.

2 Materials and Methods

2.1 Body Movement Measurements

Body movements of 13 healthy subjects and 12 patients with PD were measured. The thirteen healthy subjects were from Tsinghua University, and none of them experienced insomnia, hypersomnia, or other sleep disorders. All experimental procedures on the healthy subjects were approved by the University Committee on Research Practice at Tsinghua University. The twelve patients with PD were enrolled from Beijing Tiantan Hospital and Peking Union Medical College Hospital. Six of the patients had just had DBS implantation surgery with the implantable pulse generator in the OFF mode (DBS OFF), while the other six patients had implantable pulse generators that were turned on (DBS ON). All the PD patients suffered from one or more motor symptoms, including rigidity and tremors. The information of the subjects is shown in Table 1. All the healthy subjects and patients were informed about the entire experiment and were free to quit at any time. They all signed an informed consent form. The tests conducted on the patients with PD were approved by the Beijing Tiantan Hospital Medical Ethics Committee and the Peking Union Medical College Hospital Medical Ethics Committee.

The data collection procedure for each subject lasted 9 h at night, including the time before going to bed, in bed, and getting up the next morning. During the 9 h, the subjects were required to attach a detection device to the skin of the non-dominant wrist and the chest below the clavicle. Each subject was also monitored using an infrared camera during the 9 h. The wake/sleep state of each subject for each time period was obtained from the video recordings. Each subject or the accompanying family members were asked to recall the wake/sleep states the following morning. They were also asked to do a self-rating of sleep. With these methods, a relatively real standard wake/sleep state was obtained as the criterion to evaluate the algorithm performance.

The effectiveness of video recordings as the criterion for the wake/sleep state has been previously demonstrated. Several studies have used video recordings to record subjects' behavioral states to obtain a standard for the wake/sleep state [16, 17]. Scatena et al. [18] reported that video recordings can be used as the criterion for wake/sleep analyses and this could be particularly useful in clinical and experimental settings in which traditional PSD could not be performed. Video is superior to PSG, which typically requires a fixed experimental environment and strict constraints on the subject. Thus, video recording is the first choice when conducting experiments on infants, patients, or animals.

The detection device used in the experiment included the sensor module, data storage module, microcontroller, and battery, with a total size of 45 mm × 11 mm × 17 mm. The acceleration data for the body movement was sampled using a single three-axis micro-accelerometer (MMA845X, Freescale Semiconductor, USA) at a sampling rate of 10 Hz, with a range of ±2 g. The 9 h of acceleration data were stored on a removable storage card. The detection device was attached to the surface of the subject's skin using a medical adhesive. Figure 1 displays the 9-h three-axis acceleration data obtained from the chest below the clavicle of one subject.

2.2 Wake/Sleep Identification Algorithms for Chest and Wrist

During the development of the algorithm for the chest location below the clavicle and the wrist, two of the nine healthy subjects were used as the training group with the other seven healthy subjects and the twelve PD patients used as the validation group.

Table 1 Subject information

	Type of subjects	No. of subjects	Age (years)	Weight (kg)
Training group	Healthy young adults	2	25.0 ± 1.0	63.8 ± 6.3
Validation group	Healthy young adults	7	24.7 ± 1.6	56.1 ± 7.6
	Healthy old people	4	61.5 ± 0.5	64.0 ± 9.5
	PD patients (DBS ON)	6	64.8 ± 2.2	59.1 ± 5.5
	PD patients (DBS OFF)	6	64.2 ± 1.8	58.1 ± 4.8

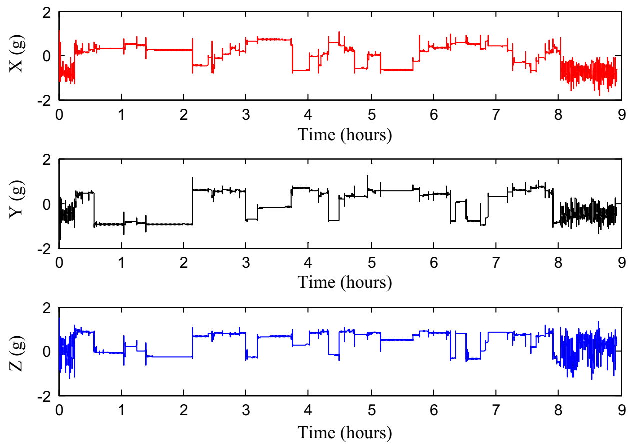

Fig. 1 Raw acceleration data from chest for one subject

Three indices were selected to evaluate the performance of the wake/sleep identification algorithm, namely accuracy, sensitivity, and specificity. Accuracy was the comprehensive index used to evaluate the algorithm. Sensitivity represents an algorithm's ability to identify the wake state, which is essential to closed-loop DBS. Specificity is less significant than sensitivity and can thus be sacrificed to get a higher sensitivity in closed-loop DBS.

$$Accuracy = \frac{TP + TN}{TP + TN + FN + FP} \tag{1a}$$

$$Sensitivity = \frac{TP}{TP + FN} \tag{1b}$$

$$Specificity = \frac{TN}{TN + FP} \tag{1c}$$

True positive (TP) is the wake state is correctly identified as the wake state. False positive (FP) is the sleep state is incorrectly identified as the wake state. True negative (TN) is the sleep state is correctly identified as the sleep state. False negative (FN) is the wake state is incorrectly identified as the sleep state.

Unlike all previous wake/sleep identification algorithms, the algorithms for the chest and the wrist were processed in real time. The algorithms for the two locations were similar, with the main difference being the analyses of the body movement characteristics for the chest, which included a posture analysis algorithm. The algorithm flow chart for the chest is shown in Fig. 2.

2.2.1 *Step 1: Calculation of Activity Intensity*

The activity intensity during each period has been defined in different ways, such as zero crossing mode (ZCM), proportional integral mode (PIM), and time above threshold (TAT). Different definitions are used in different algorithms for different situations. The wrist algorithm uses ZCM to calculate the activity intensity because it is very simple and best reflects the intense movements of the wrist. The activity intensity for each period for the wrist is defined as the number of times the acceleration crossed zero during each period (30 s). The waveform of activity intensity in Fig. 3a was calculated according to the raw acceleration data for the wrist algorithm. Figure 3a was also used in our previous publication [19], which did not present the details of the detection algorithm. The chest algorithm uses PIM to calculate the activity intensity. The activity intensity of each period, A, for the chest was calculated as:

$$A = \frac{1}{T}\left(\int_0^T |x(t)|\, dt + \int_0^T |y(t)|\, dt + \int_0^T |z(t)|\, dt \right) \tag{2}$$

where $x(t)$, $y(t)$, and $z(t)$ represent the three axis accelerations, respectively, and T is the time span of each period. The waveform of the activity intensity in Fig. 3b is calculated for the chest algorithm.

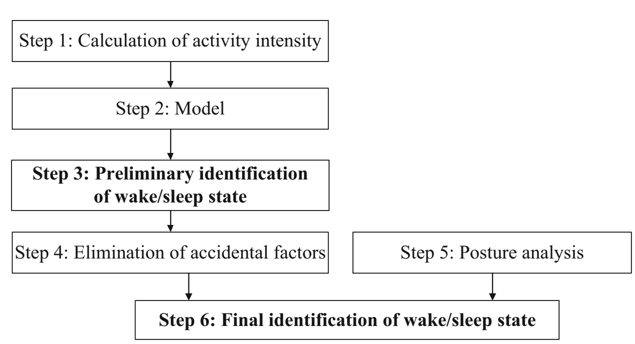

Fig. 2 Algorithm flow chart for chest measurement

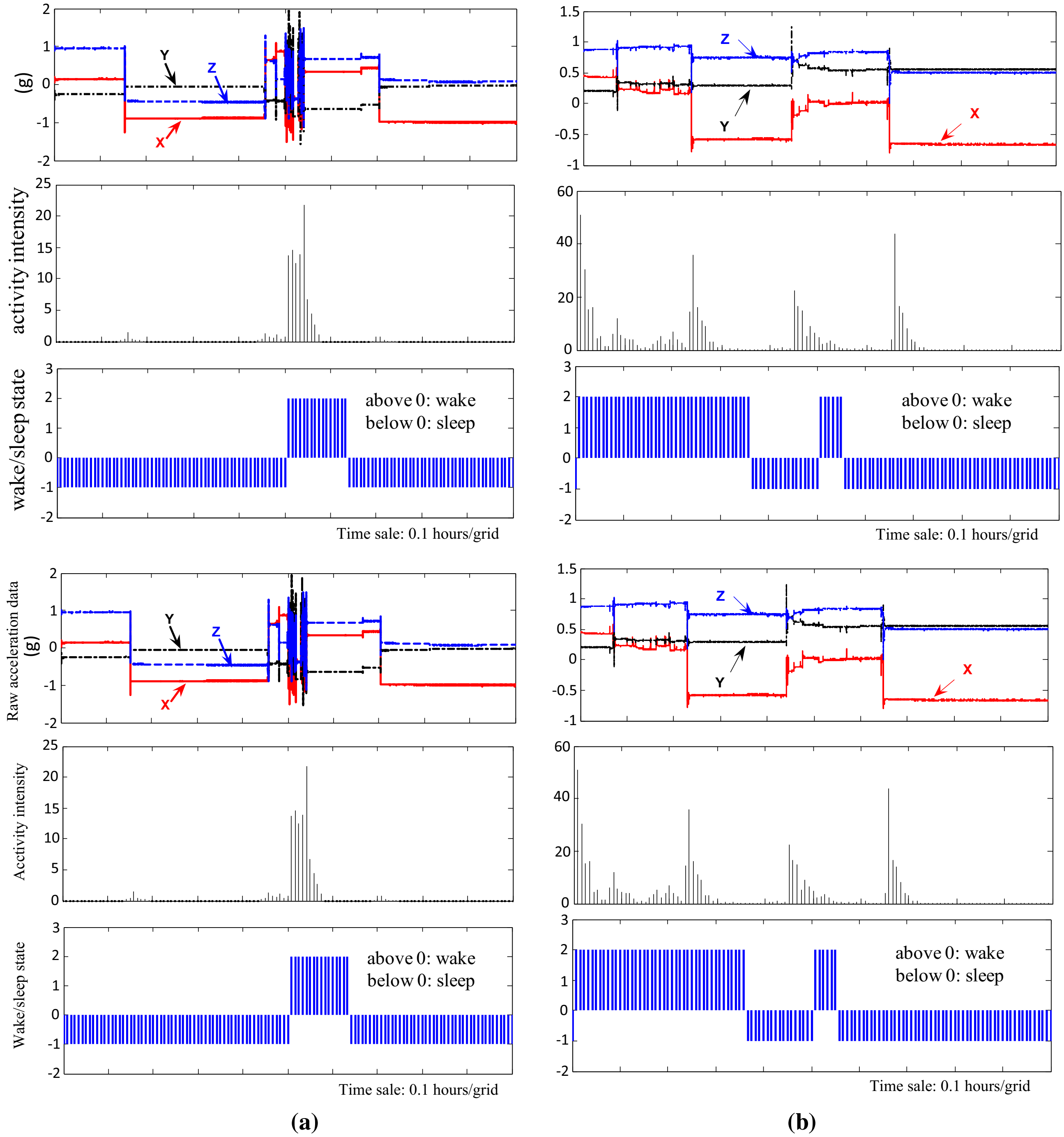

Fig. 3 Raw acceleration data, activity intensity, and identified states during 1 h for **a** wrist algorithm and **b** chest algorithm

2.2.2 Step 2: Model

The relationship between the activity intensity and the wake/sleep state is defined using a logistic regression model, which typically deals with the relationship between consecutive independent variables (X) and a two-value dependent (Y) variable. The wake/sleep state (Y) is defined as:

$$Y = \begin{cases} 1 & \textit{wake state} \\ 0 & \textit{sleep state} \end{cases} \tag{3}$$

For the logistic regression model, the relationship between the probabilities of Y and X is:

$$\pi(X) = P(Y = 1|X) \tag{4}$$

In general, there are no abrupt body movements, so the wake/sleep state can be related to the combinations of the activity intensity for several previous periods. The model describing the relationship between the activity intensity and wake/sleep state is:

$$\pi(A) = \omega_{-n}A_{-n} + \cdots + \omega_{-2}A_{-2} + \omega_{-1}A_{-1} + \omega_0 A_0 \quad (5)$$

where A_{-i} is the activity intensity of each period, where "$-$" indicates the previous periods, $\omega_{-\mathrm{i}}$ is the scale of activity intensity, A_{-i}, n is the number of previous periods taken into consideration.

The parameters in Eq. (5) were determined using maximum likelihood estimation. The value of n was selected by analyzing the accuracy of the wake/sleep identification. Figure 4 shows the relationship between n and accuracy. The accuracy increases with n when n is below 4, and decreases for n above 4. Thus, the value of n was chosen as 4.

2.2.3 *Step 3: Preliminary Identification of Wake/Sleep State*

The wake/sleep state was identified by setting a threshold, π_{th}, for the model in Eq. (5). When $\pi(A) > \pi_{th}$, the state is identified as wake; otherwise, the state is identified as sleep. The threshold, π_{th}, reflects the probability of the wake state and the sleep state when the body movement is at a specific activity intensity; thus, π_{th} was set to 0.5.

2.2.4 *Step 4: Elimination of Accidental Factors*

Webster et al. [10] proposed a series rescoring method for their non-real-time algorithm. The proposed real-time wake/sleep identification algorithm uses the following rescoring method to eliminate accidental factors. (1) When the current period is identified as a sleep state, if all seven previous periods were identified as wake, then the current period is re-identified as a wake state. (2) When the current period is identified as a wake state, if all seven previous periods were identified as sleep, then the current period is re-identified as a sleep state. (3) The re-identified state is labeled differently from the other identified states (not changed during the rescoring process) and is not considered in the next rescoring process.

The identified wake/sleep state for the wrist algorithm in Fig. 3a is plotted for a duration of 1 h. The segment above 0 is for the wake state, and that below 0 is for the sleep state. The identified state was updated in each period (30 s).

The efficacy of step four is demonstrated in Fig. 5. The red line represents the real state. Figure 5a, b show the difference between the identification results before and after step four (elimination of accidental factors), respectively. The lower segments (-1.5) represent the subject's sleep state, obtained from the video recordings. Eliminating accidental factors corrected some wrongly identified periods.

2.2.5 *Step 5: Posture Analysis (Only Applicable for Chest Algorithm)*

Typically, the posture of an individual during sleep is prone, supine, or lateral. Thus, the subject's posture can also be used for wake/sleep identification. A more reliable indication of the wake/sleep state was formed by analyzing the preliminarily wake/sleep state identification using posture analysis.

Figure 6 shows the orientation of the three-axis micro-accelerometer with respect to the human body. For the ideal situation, the X, Y, and Z axes are aligned with the

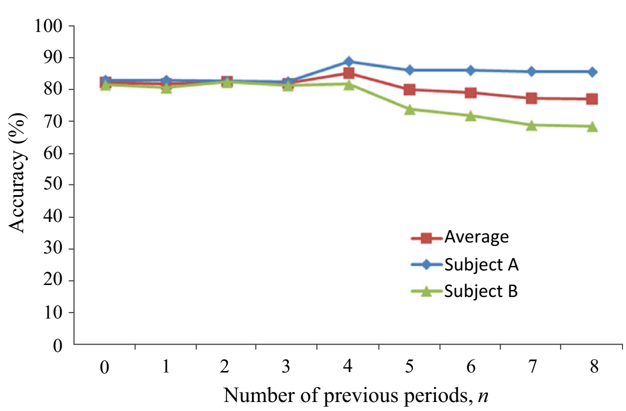

Fig. 4 Relationship between n and accuracy (%)

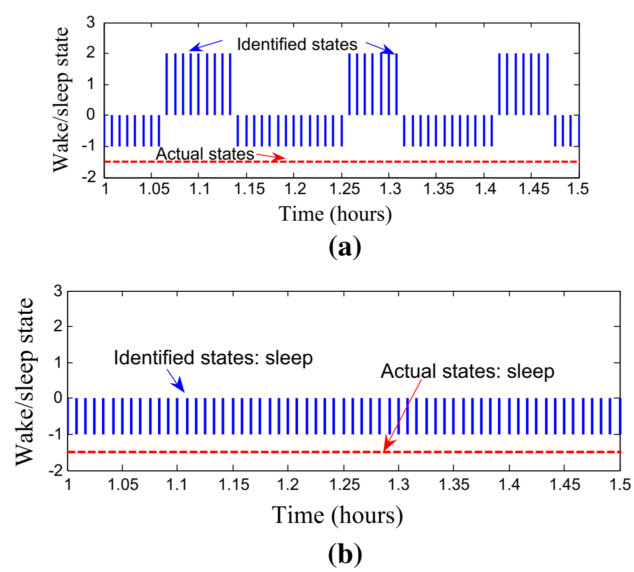

Fig. 5 Examples of identification results **a** before and **b** after elimination of accidental factors (step four)

vertical, horizontal, and anterior-posterior directions, respectively. However, the angles are neither equal to zero nor remain constant for each attachment of the detection device on the skin. These angles are represented with $\theta(pitch)$, $\varphi(roll)$, and $\psi(yaw)$ respectively.

The subject's posture is obtained by first calculating the angles between the three axes of the accelerometer and the human body, namely $\theta_0(pitch)$, $\varphi_0(roll)$, and $\psi_0(yaw)$. Then, three thresholds are set for the three angles between the three axes of the accelerometer and the inertial frame, namely $\theta_{TH}(pitch)$, $\varphi_{TH}(roll)$, and $\psi_{TH}(yaw)$. The "up" posture and the "lying" posture are then obtained via comparison.

A three-dimensional rotation can be defined as yaw → roll → pitch with the transition matrix:

$$R_yR_zR_x = \begin{bmatrix} \cos\theta\cos\varphi & \cos\theta\sin\varphi\cos\psi + \sin\theta\sin\psi & \cos\theta\sin\varphi\sin\psi - \sin\theta\cos\psi \\ -\sin\varphi & \cos\varphi\cos\psi & \cos\varphi\sin\psi \\ \sin\theta\cos\varphi & \sin\varphi\sin\theta\cos\psi - \sin\psi\cos\theta & \sin\varphi\sin\theta\sin\psi + \cos\theta\cos\psi \end{bmatrix} \tag{6}$$

Assume that the three axis accelerations for the standing posture are $[x' \quad y' \quad z']^T$ and those for the supine posture are $[x'' \quad y'' \quad z'']^T$. These values can be obtained when the subject is in a known posture (e.g., standing or supine). For the ideal situation, these two sets of accelerations should be $[-1 \quad 0 \quad 0]^T$ and $[0 \quad 0 \quad 1]^T$, respectively. The two possible transitions are:

$$\begin{bmatrix} x' \\ y' \\ z' \end{bmatrix} = R_yR_zR_x \begin{bmatrix} -1 \\ 0 \\ 0 \end{bmatrix} \quad \begin{bmatrix} x'' \\ y'' \\ z'' \end{bmatrix} = R_yR_zR_x \begin{bmatrix} 0 \\ 0 \\ 1 \end{bmatrix} \tag{7}$$

These equations can be solved to get the three angles $\theta_0(pitch)$, $\varphi_0(roll)$, and $\psi_0(yaw)$.

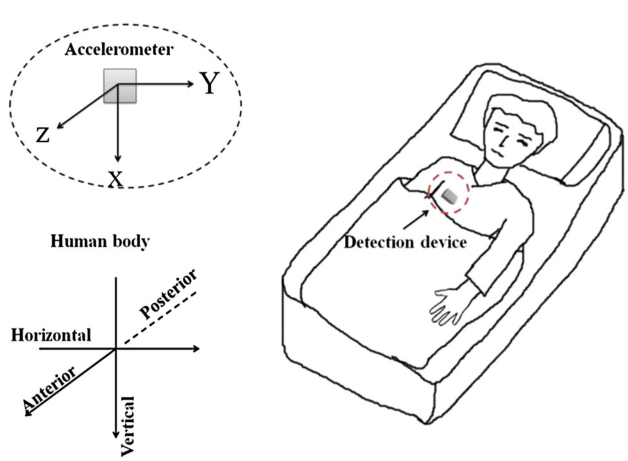

Fig. 6 Orientation of accelerometer relative to human body

$$roll: \varphi_0 = \arcsin(y') \tag{8a}$$

$$yaw: \psi_0 = \arcsin\left(\frac{y''}{\cos\varphi}\right) \tag{8b}$$

$$pitch: \theta_0 = \arccos\left(-\frac{x'}{\cos\varphi}\right) \; or \; \theta_0 = \arcsin\left(-\frac{z'}{\cos\varphi}\right) \tag{8c}$$

After thresholds $\theta_{TH}(pitch)$, $\varphi_{TH}(roll)$, and $\psi_{TH}(yaw)$ have been set, when the acceleration for an arbitrary posture satisfies these expressions, the posture is "up"; otherwise, it is "lying".

$$\begin{cases} |x| > Mag \cdot \cos(\theta_0+\theta_{TH}) \\ |y| < Mag \cdot \sin(\varphi_0+\varphi_{TH}) \\ |z| < Mag \cdot \sin(\theta_0+\theta_{TH}) \end{cases} \quad Mag = \sqrt{x^2+y^2+z^2} \tag{9}$$

These expressions can be written as:

$$\begin{aligned} &\text{if } \{\bar{x} > -Mag \times \cos(\theta_0+\theta_{TH}) \text{ and } (|\bar{y}| > Mag \\ &\quad \times \sin(\varphi_0+\varphi_{TH}) \text{ or } |\bar{z}| > Mag \times \sin(\theta_0+\theta_{TH}))\}, \\ &then\ the\ lying\ posture;\ otherwise,\ the\ up\ posture. \end{aligned} \tag{10}$$

There were 300 posture measurements for each period (30 s). If 60 % of the results were "up", the posture for that period was set to "up"; otherwise, the posture was "lying".

2.2.6 *Step 6: Final Identification of Wake/Sleep State for Chest Algorithm*

The final wake/sleep state is generated from a combined analysis of the results of steps four and five.

Figure 7 shows the process used to determine the final wake/sleep state, which is a comprehensive analysis of eliminating accidental factors and posture analysis. Y(0) represents the wake/sleep state of the current period, and Y(−i) represents the wake/sleep state of the previous period. The preliminary identification of the wake/sleep state is modified according to the wake/sleep states of the previous periods and the posture of the current period. The

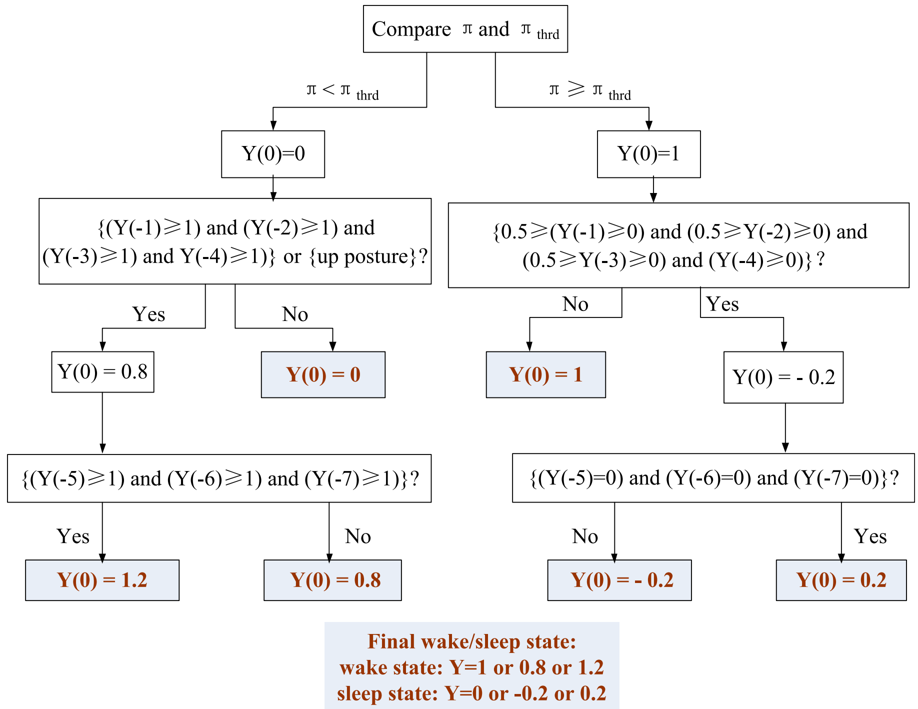

Fig. 7 Process for calculating final wake/sleep state in chest algorithm

value of Y(0) is modified from 0, representing the sleep state (or 1, representing the wake state), to 0.8 (or -0.2) when the previous four periods are all the wake state or the current posture is "up" (or the previous four periods are all the sleep state). Furthermore, if all the previous seven periods are the wake state (or all the sleep state), Y(0) is modified to 1.2 (or 0.2). The final state is identified as the wake (sleep) state when Y(0) = 1, 0.8, or 1.2 (0, -0.2, or 0.2). The values of -0.2 and 0.8 indicate that the modification has lower reliability, whereas 0.2 and 1.2 indicate that the modification has higher reliability.

The identified wake/sleep state for the chest algorithm in Fig. 3b is plotted for a time duration of 1 h. The segment above 0 is the wake state, and that below 0 is the sleep state. The identified state was updated for each period (30 s).

The efficacy of posture analysis is demonstrated in Fig. 8, which shows two examples that show the difference between the identification results before and after step six. The higher and lower segments (+2.5 and -1.5) represent the subject's wake and state states, respectively, obtained from the video recordings. The posture analysis corrected most of the incorrectly identified periods when the subject was "sitting and reading" or was "on the bed and awake". One result is that more periods were identified or misidentified as the wake state, which gives a higher sensitivity, as shown in Fig. 8b, d. Note that a higher sensitivity with less specificity is better for the wake/sleep identification algorithm for PD patients because the consequence of delivering stimulation to patients when periods are misidentified as the wake state is not as serious as withholding stimulation when periods are misidentified as the sleep state. The stimulation is to be delivered continuously while the patient is awake.

2.3 Analysis of Wake/Sleep Identification Algorithm After Each Step

Acceleration data of the training group was used to determine the wake/sleep identification algorithms for the chest and the wrist. The parameters in the algorithms were determined when the identified wake/sleep states agreed with the actual states at the highest accuracy. The parameters of the model in Eq. (5) for the wrist and the chest are respectively:

$$\pi(A) = P(Y = 1|\textit{wrist activity intensity}) = \frac{1}{54}(A_{-4} + 2 \times A_{-3} + 5 \times A_{-2} + 8 \times A_{-1} + 11 \times A_0) \tag{11}$$

$$\pi(A) = P(Y = 1|\textit{chest activity intensity}) = \frac{1}{50}(A_{-4} + 2 \times A_{-3} + 3 \times A_{-2} + 4 \times A_{-1} + 15 \times A_0) \tag{12}$$

Figure 9 shows an example of the 9-h wake/sleep identification using the chest algorithm for one subject. The identified wake/sleep state is plotted for each period, and

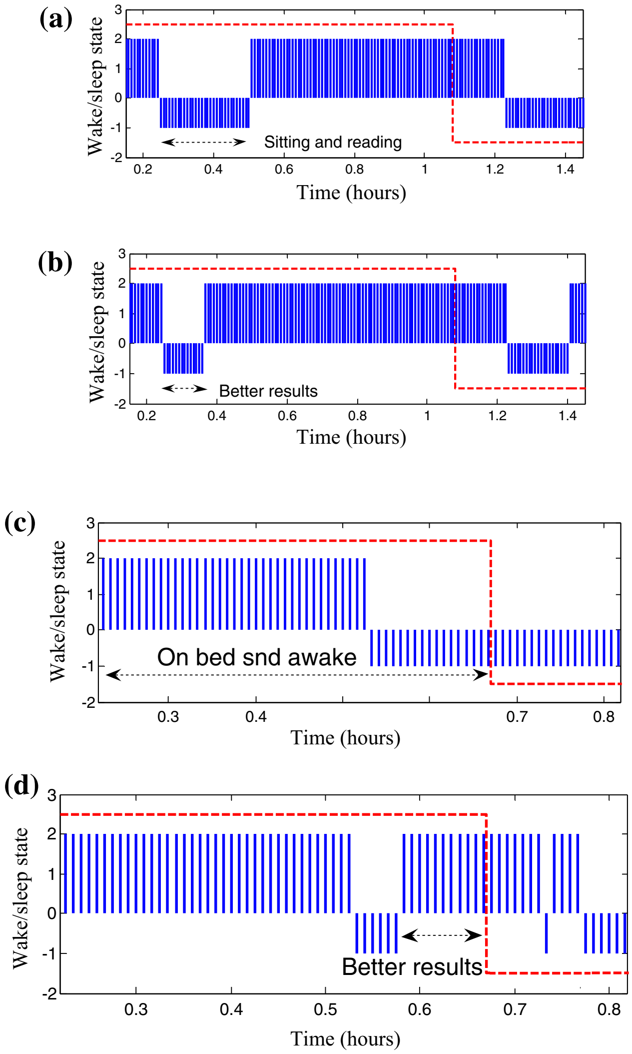

Fig. 8 Examples of results **a**, **c** before and **b**, **d** after final identification of wake/sleep state (step six)

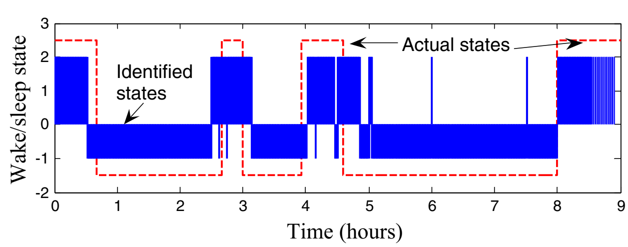

Fig. 9 Nine-hour wake/sleep identification results obtained using chest algorithm

the actual states obtained from the video recordings are plotted as well. The identified state (the segment above 0) represents the wake state of each period, and the identified state (the segment below 0) represents the sleep state of each period. The actual states are represented by the higher and lower segments (+2.5 and −1.5).

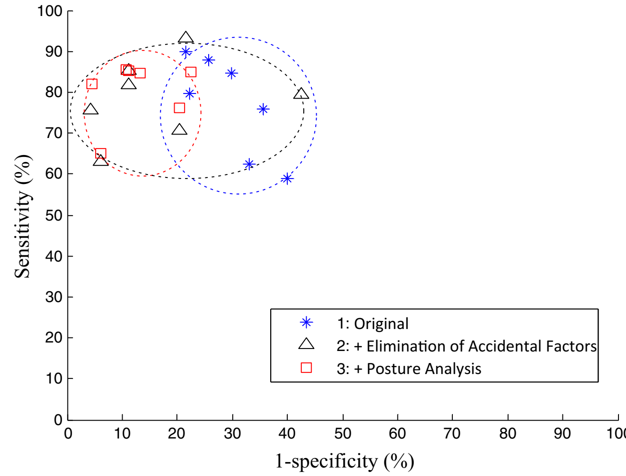

Fig. 10 Performance of each step in algorithm

The efficacy of the wake/sleep identification algorithm was also analyzed statistically. The data from the seven healthy young subjects in the validation group were used to analyze the performance of the algorithm after step three (preliminary wake/sleep state identification), step four (elimination of accidental factors), and step five (posture analysis). Figure 10 compares the sensitivity and specificity after each step. The three symbols represent the performance after step three (*), step four (△), and step five (□). The symbols move towards the upper left as the algorithm proceeds, demonstrating the efficacy of each step.

3 Results

The real-time wake/sleep identification algorithms for the chest and wrist were validated on both healthy subjects and PD patients. Table 2 shows the statistical results for the healthy subjects, with the average accuracy, sensitivity, and specificity calculated for the wrist and the chest. All the indices are higher than 70 % in the healthy subject validation group. These real-time algorithms achieved performance comparable to that of previous wake/sleep identification studies [5, 20].

A comparison of the algorithms for the wrist and the chest shows that the chest algorithm has better statistical results. In both the training group and validation group, the average accuracy for the chest is higher than those for the wrist. For the indices of average sensitivity and specificity, the results for the chest and the wrist are roughly comparable, while the average sensitivity for the chest is more concentrated than that for the wrist. This implies a more stable performance of the algorithm for the chest location.

Table 3 shows the statistical results for the twelve PD patients, six of which had stimulation turned OFF and six

Table 2 Statistical results for young and old subjects

Location	No. of subjects	Actual state	Identified state		Mean ± SD (%)		
			Wake	Sleep	Acc.	Sen.	Spe.
Wrist	Training: 2	Wake	339[a]	48	**83.06**	**87.60**	**82.06**
		Sleep	318	1455	±0.84	±5.21	±0.10
	Validation: young 7	Wake	1365	550	**82.41**	**71.28**	**86.18**
		Sleep	780	4865	±3.24	±14.20	±3.69
	Old 4	Wake	1874	352	**81.78**	**84.19**	**79.23**
		Sleep	435	1659	±6.45	±15.83	±2.69
Chest	Training: 2	Wake	669	70	**84.68**	**90.50**	**81.69**
		Sleep	261	1160	±1.69	±3.64	±3.14
	Validation: young 7	Wake	1554	352	**85.95**	**81.53**	**87.44**
		Sleep	710	4944	±4.26	±7.32	±5.15
	Old 4	Wake	482	179	**82.89**	**72.92**	**84.70**
		Sleep	560	3099	±1.50	±3.37	±2.17

[a] Unit: Number of periods (30 s/period)

Table 3 Algorithm performance for PD patients

Condition	Location	Accuracy (%)	Sensitivity (%)	Specificity (%)
DBS OFF	Wrist	82.45 ± 9.17	75.58 ± 10.15	82.79 ± 12.06
	Chest	82.74 ± 6.00	82.68 ± 10.50	82.28 ± 9.12
DBS ON	Wrist	80.32 ± 4.63	75.26 ± 11.96	84.73 ± 8.21
	Chest	85.78 ± 7.80	84.21 ± 10.69	82.08 ± 8.69

of which had stimulation turned ON. From The three performance indices are all higher than 75 % for both the chest and the wrist. Thus, the real-time wake/sleep identification algorithm gives good performance for the PD patients. In addition, the chest indices are all higher than 80 % and all higher than those for the wrist, which again demonstrates the good performance of the algorithm for the chest.

The influence of DBS on the algorithm performance was studied by dividing the PD patients into DBS ON and DBS OFF groups. From Table 3, when DBS was OFF, the sensitivity was 82.68 %, which means that the algorithm correctly identified the wake state and the stimulation was turned on during the wake state. When DBS was ON, the specificity was 82.08 %, which means that the algorithm correctly identified the sleep state and the stimulation was turned off. The good performance in both the DBS ON and DBS OFF scenarios shows that closed-loop DBS should be effective.

The proposed real-time wake/sleep identification algorithm has good performance, with high accuracy, sensitivity, and specificity. This real-time algorithm has accuracy comparable to that of previous non-real-time wake/sleep identification algorithms. Sazonov et al. [20] reported accuracies of 77–92 % for the wake/sleep state of infants with a detection device on the diaper. Watanabe [5] demonstrated a noncontact pneumatic method for sleep stage estimation that had a 70.5 % identification rate of the wake state. The present study is the first to identify the wake/sleep state by measuring body movement at the chest below the clavicle.

The proposed wake/sleep identification algorithm is very flexible, which promises good performance for a wide range of subjects. Several parameters in the algorithm can be modified to provide flexibility, such as the π_{thrd} threshold for $\pi(A)$ and thresholds for the three angles in step five (posture analysis). Different subjects can have different θ_{TH}, φ_{TH}, and ψ_{TH} thresholds for their typical "up" and "lying" postures. This algorithm is also applicable for different types of subject, including healthy young adults and PD patients with DBS ON or OFF.

4 Discussion

This study demonstrated a simple, reliable method for identifying wake/sleep states based on body movements from the chest below the clavicle. Body movement identification has several advantages over EEG feedback. One is that identification based on body movements has high accuracy (91–93 %) [15], comparable to that obtained using PSG. The second advantage is that the body movement method makes no additional constraints on the subject's daily activities. The subject only needs to wear a small detection device, which does not interfere with the subject's daily life. The PSG method is more complex, with EEG requiring multiple electrodes on the scalp and a heavy restraint over the subjects. The third advantage is that the great progress in microelectromechanical systems allows detection device miniaturization. Various micro inertial sensors with many features, such as accelerometers and gyroscopes, are widely used to measure body movements. These developments in the underlying technologies are leading to rapid progress in implantable medical devices. The small size and simple design of the sensor module presented in this study make it applicable to a closed-loop deep brain stimulator based on wake/sleep identification.

The results demonstrate better performance of the algorithm on the chest. These results suggest the feasibility of closed-loop DBS with a wake/sleep identification module implanted subcutaneously in the chest, feeding directly into the pulse generator. Furthermore, the chest location has higher sensitivity. Since the sensitivity describes the ability of the algorithm to correctly identify the wake state, the algorithm for the chest location is more suitable for closed-loop DBS.

Most importantly, this study shows the importance of the closed-loop deep brain stimulator design. The excellent performance of the real-time wake/sleep identification algorithm for the chest location is promising for future closed-loop DBS applications. The wake/sleep identification module can be designed directly into the implantable pulse generator, with the stimulations adapting automatically to the patient's wake/sleep state. For example, when the patient is in the sleep state, the stimulation is turned off or the stimulation amplitude is reduced; when the patient is in the wake state, the stimulation is turned on.

Other issues related to the efficacy of the closed-loop DBS should be taken into account in future research. Firstly, the performance of the algorithm on patients with rigidity should be analyzed. Different from tremors, it is difficult to use actigraphy to differentiate rigidity and the sleep state. Further validation should be carried out. For example, subjects could be divided into two categories, those with rigidity and those with tremors. Secondly, the influence of the delayed electrical stimulation mode should be carefully studied. The delay time of the algorithm should be controlled to be in a specific range. The delayed action of turning DBS on or off should also be studied before putting closed-loop DBS into use.

The proposed method can also be implemented in other medical devices. For example, with a wireless communication module, the wake/sleep identification can trigger an alarm to deal with an emergency at night. This is extremely useful for nurses watching patients with movement disabilities during the night. The accelerometer-based system can also be used to detect falls of the elderly and sound an alarm for help.

There are some limitations in this study. First, the results were not compared with those obtained using PSG because of the inconvenience for the PD patients in the hospital. Video was used as the evaluation criterion instead, which is accurate but slightly less so than PSG. The memories of the wake/sleep states in the last night of the subjects themselves or their accompanying family members were referenced. The subjects were also asked to use a self-rating scale of sleep the following morning. Second, the real-time wake/sleep identification algorithm for the chest data includes posture analysis based on the movement of the chest below the clavicle. It is important to get the exact pitch, roll, and yaw angles to compute the posture state. The device was not equipped with a gyroscope, which could be used to directly derive the pitch, roll, and yaw angles for comparison with the calculated posture angle. In the posture analysis process, the angle threshold for each individual is required because its value for the body "up" or "lay" posture varies with subject. The results show that the posture analysis proved conducive to the judgment and improved the wake/sleep state detection accuracy.

5 Conclusion

This study demonstrated real-time wake/sleep identification algorithms for the chest and the wrist. The algorithms were tested on both healthy adults and PD patients to show their effectiveness. The accuracy, sensitivity, and specificity for the chest location were all higher than 80 %, which is comparable to results reported in other studies. This research provides a practical method for closed-loop deep brain stimulators, which will greatly benefit patients with PD.

Acknowledgments This work was supported by NSFC (51125028), the Tsinghua University Initiative Scientific Research Program, and the National Key Technology Research and Development Program (2012BAI16B01).

References

1. Kringelbach, M. L., Jenkinson, N., Owen, S., & Aziz, T. Z. (2007). Translational principles of deep brain stimulation. *Nature Reviews Neuroscience, 8*, 623–635.
2. Chuang, W. Y., Chao, P. C. P., & Young, K. Y. (2014). computerized stimulation parameter adjustment of deep brain stimulation minimizing side effects and power consumption for Parkinson's disease. *Journal of Medical and Biological Engineering, 34*, 310–318.
3. Moro, E., Esselink, R., Xie, J., Hommel, M., Benabid, A. L., & Pollak, P. (2002). The impact on Parkinson's disease of electrical parameter settings in STN stimulation. *Neurology, 59*, 706–713.

4. Jankovic, J. (2008). Parkinson's disease: clinical features and diagnosis. *Journal of Neurology, Neurosurgery and Psychiatry, 79*, 368–376.
5. Watanabe, T., & Watanabe, K. (2004). Noncontact method for sleep stage estimation. *IEEE Transactions on Biomedical Engineering, 51*, 1735–1748.
6. Flores, A. E., Flores, J. E., Deshpande, H., Picazo, J. A., Xie, X., Franken, P., et al. (2007). Pattern recognition of sleep in rodents using piezoelectric signals generated by gross body movements. *IEEE Transactions on Biomedical Engineering, 54*, 225–233.
7. Okada, S., Ohno, Y., Goyahan, Kato-Nishimura, K., Mohri, I., & Taniike, M. (2008). Examination of non-restrictive and non-invasive sleep evaluation technique for children using difference images. In *30th IEEE-EMBS* (Vol. 1–8, pp. 3483–3487).
8. Pollak, C. P., Tryon, W. W., Nagaraja, H., & Dzwonczyk, R. (2001). How accurately does wrist actigraphy identify the states of sleep and wakefulness? *Sleep, 24*, 957–965.
9. Shinkoda, H., Matsumoto, K., Hamasaki, J., Seo, Y. J., Park, Y. M., & Park, K. P. (1998). Evaluation of human activities and sleep-wake identification using wrist actigraphy. *Psychiatry and Clinical Neurosciences, 52*, 157–159.
10. Webster, J. B., Kripke, D. F., Messin, S., Mullaney, D. J., & Wyborney, G. (1982). An activity-based sleep monitor system for ambulatory use. *Sleep, 5*, 389–399.
11. Cole, R. J., Kripke, D. F., Gruen, W., Mullaney, D. J., & Gillin, J. C. (1992). Automatic sleep wake identification from wrist activity. *Sleep, 15*, 461–469.
12. Dick, R., Penzel, T., Fietze, I., Partinen, M., Hein, H., & Schulz, J. (2010). AASM standards of practice compliant validation of actigraphic sleep analysis from SOMNOwatch™ versus polysomnographic sleep diagnostics shows high conformity also among subjects with sleep disordered breathing. *Physiological Measurement, 31*, 1623–1633.
13. Hedner, J., Pillar, G., Pittman, S. D., Zou, D., Grote, L., & White, D. P. (2004). A novel adaptive wrist actigraphy algorithm for sleep-wake assessment in sleep apnea patients. *Sleep, 27*, 1560–1566.
14. Tilmanne, J., Urbain, J., Kothare, M. V., Wouwer, A. V., & Kothare, S. V. (2009). Algorithms for sleep-wake identification using actigraphy: a comparative study and new results. *Journal of Sleep Research, 18*, 85–98.
15. Sadeh, A., Sharkey, K. M., & Carskadon, M. A. (1994). Activity-based sleep-wake identification - an empirical test of methodological issues. *Sleep, 17*, 201–207.
16. Carroll, D. A., Denenberg, V. H., & Thoman, E. B. (1993). Reliability and validity of computer scoring of behavioral sleep-wake states in rats and rabbits. *Physiology & Behavior, 54*, 269–273.
17. Thoman, E. B., & Tynan, W. D. (1979). Sleep states and wakefulness in human infants—Profiles from motility monitoring. *Physiology & Behavior, 23*, 519–525.
18. Scatena, M., Dittoni, S., Maviglia, R., Frusciante, R., Testani, E., Vollono, C., et al. (2012). An integrated video-analysis software system designed for movement detection and sleep analysis. Validation of a tool for the behavioural study of sleep. *Clinical Neurophysiology, 123*, 318–323.
19. Chen, Y., Hao, H. W., Hu, Y. X., & Li, L. M. (2013). Wireless wrist-wearable wake/sleep identification device for closed-loop deep brain stimulation. *Electronics Letters, 49*, 452–453.
20. Sazonov, E., Sazonova, N., Schuckers, S., & Neuman, M. (2004). Activity-based sleep-wake identification in infants. *Physiological Measurement, 25*, 1291–1304.